Kinetics and Mechanism of Phosphine Autoxidation Catalyzed by Imidorhenium(V) Complexes

Wei-Dong Wang and James H. Espenson*

Ames Laboratory and Department of Chemistry, Iowa State University of Science and Technology, Ames, Iowa 50011

Received August 16, 2000

The relative binding abilities of PY_3 (PMe_3, PMe_2Ph, $PMePh_2$, PPh_3, $P(OMe)_3$, $P(OMe)_2Ph$, PEt_3, $P(OEt)_3$, $P(OEt)Ph_2$, and dmpe) toward Re^V were evaluated. The equilibrium constants for the reactions, $MeRe(NAr)_2\{P(OMe)_3\}_2 + PY_3 = MeRe(NAr)_2(PY_3)_2$ (**1**) + $P(OMe)_3$, decrease in the order PMe_3 > dmpe > PMe_2Ph > $P(OMe)_2Ph$ ∼ PEt_3 > $P(OEt)_3$ > $PMePh_2$ > $P(OEt)Ph_2$ > PPh_3. Both electronic and steric factors contribute to this trend. The equilibrium constant increases as the basicity of PY_3 increases when the steric demand is the same. However, steric effects play a major role in the coordination, and this is the reason that the affinity of PEt_3 toward Re^V is less than that of PMe_2Ph. A mixed-ligand complex, $MeRe(NAr)_2\{P(OMe)_3\}(PY_3)$, was also observed in the course of the stepwise formation of **1**. The large coupling constant, $^2J_{PP} \geq 491$ Hz, between the two phosphorus atoms suggests a trans geometry for the phosphines. Compound **1** catalyzes the oxidation of PY_3 by molecular oxygen. Kinetic studies suggest that the reaction of **1** with O_2 is first-order with respect to $[O_2]$ and inverse-first-order with respect to $[PY_3]$. A mechanism involving a peroxorhenium intermediate $MeRe(NAr)_2(\eta^2\text{-}O_2)$ is proposed for the catalytic processes. The reactivity of $MeRe(NAr)_2(\eta^2\text{-}O_2)$ toward triaryl phosphines parallels that of the known compound $MeReO_2(\eta^2\text{-}O_2)$.

Introduction

Activation of molecular oxygen has attracted considerable interest because of the fundamental and practical implications in chemical as well as in biological sciences. Metal-catalyzed oxidation reactions of organic substrates still present challenges in the field of basic research.[1−3] It is known that methyltrioxorhenium, $MeRe^{VII}O_3$ or MTO, catalyzes the oxidation of phosphines with O_2, Scheme 1.[4] The first step of this inefficient process involves the formation of an intermediate Re^V species that then reacts with O_2 to yield an η^2-peroxo complex, $MeReO_2(\eta^2\text{-}O_2)$. This is an independently known species whose oxo-transfer capability has been extensively studied.[5,6] Owing to the slowness of the first step and the complexity of the system, information about the kinetics and mechanism for the O_2-reaction step is lacking. We have prepared and characterized a series of Re^V complexes, $MeRe(NAr)_2(PY_3)_2$ (Ar = 2,6-diisopropylphenyl; $PY_3 = PR_nPh_{3-n}$, $P(OR)_nPh_{3-n}$, and dmpe, Chart 1),[7] and here we would like to report their properties as catalysts for the oxidation of phosphines with O_2. We have uncovered evidence for the involvement of an η^2-peroxo intermediate, $MeRe(NAr)_2(\eta^2\text{-}O_2)$, which is analogous to the known complex $MeReO_2(\eta^2\text{-}O_2)$.

Chart 1. Structural Formulas of Rhenium(V) Compounds

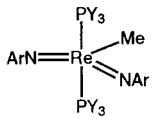

1

1a PMe_2Ph **1e** $P(OEt)_3$
1b $P(OMe)Ph_2$ **1f** PMe_3
1c $P(OMe)_2Ph$ **1g** PEt_3
1d $P(OMe)_3$ **1h** dmpe

Scheme 1

$$MeReO_3 + P(Tol)_3 \rightarrow MeReO_2 + (Tol)_3PO$$

$$MeReO_2 + O_2 \rightarrow MeReO_2(\eta^2\text{-}O_2)$$

$$MeReO_2(\eta^2\text{-}O_2) + P(Tol)_3 \rightarrow MeReO_3 + (Tol)_3PO$$

Experimental Section

Materials and Instruments. Phosphines were purchased from Aldrich or Strem and used without further purification. Benzene (Fisher), benzene-d_6, and toluene-d_8 (CIL) were dried with sodium/benzophenone and stored in an N_2-filled glovebox. Compound **1**, $MeRe(NAr)_2(PY_3)_2$, has been fully characterized including elemental analyses, NMR studies, and single-crystal X-ray determinations for $PY_3 = PMe_2Ph$ (**1a**) and $Me_2PCH_2CH_2PMe_2$ (**1h**).[7] The molecular structure of **1h** shows that the dmpe ligands coordinate to rhenium in a monodentate fashion. ^1H, $^{31}P\{^1H\}$, and ^{13}C NMR spectra were recorded using a Bruker DRX-400 spectrometer. Kinetic studies were carried out at 298 K using Shimadzu UV 3101PC and Applied Photophysics DX 17MV stopped-flow spectrophotometers.

Kinetics. A stock solution of **1** in C_6H_6 was prepared and stored under N_2. The concentration of O_2 in its saturated benzene solution is

* Author to whom correspondence should be adressed. E-mail address: espenson@iastate.edu.

(1) Simandi, L. I. *Catalytic Activation of Dioxygen by Metal Complexes*; Kluwer Academic Publishers: Dordrecht, 1992.
(2) *The Activation of Dioxygen and Homogeneous Catalytic Oxidation*; Barton, D. H. R., Martell, A. E., Sawyer, D. T., Eds.; Plenum: New York, 1993.
(3) *Active Oxygen in Chemistry*; Foote, C. S., Valentine, J. S., Greenberg, A., Liebman, J. F., Eds.; Blackie Academic & Professional: New York, 1995.
(4) Eager, M. D.; Espenson, J. H. *Inorg. Chem.* **1999**, *38*, 2533.
(5) Espenson, J. H. *Chem. Commun.* **1999**, 479.
(6) Romão, C. C.; Kühn, F. E.; Herrmann, W. A. *Chem. Rev.* **1997**, *97*, 3197.
(7) Wang, W.-D.; Guzei, I. A.; Espenson, J. H. *Organometallics*, in press.

10.1021/ic000940k CCC: $20.00
Published on Web 02/10/2001

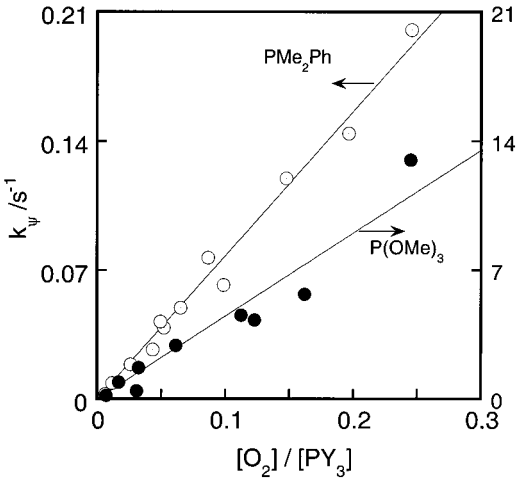

Figure 1. Plots of the pseudo-first-order rate constants for the MeRe(NAr)$_2$(PY$_3$)$_2$/O$_2$ reaction against the ratio [O$_2$]/[PY$_3$]. Solid and open circles are for PY$_3$ = P(OMe)$_3$ and PMe$_2$Ph, respectively.

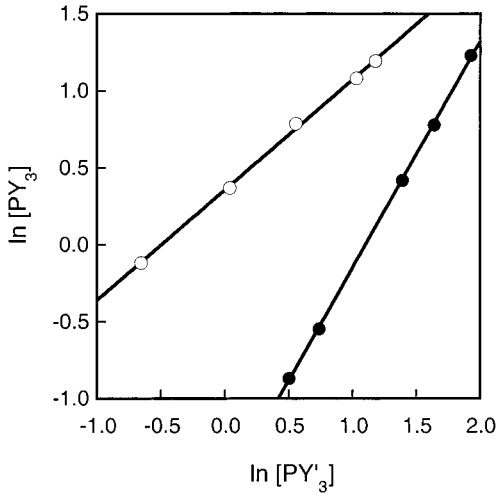

Figure 2. Data for competition kinetics for the reactions of a pair of phosphines with oxygen in the presence of a catalytic quantity of MeRe(NAr)$_2$PY$_3$. (a) The plot of ln [P(4-MeOC$_6$H$_4$)$_3$] against ln [P(4-MeC$_6$H$_4$)$_3$], solid circles. (b) The plot of ln [P(4-CF$_3$C$_6$H$_4$)$_3$] against ln [P(4-ClC$_6$H$_4$)$_3$], open circles. The intensities of the ^{31}P resonances were directly used.

9.1 mM.[8] The kinetics of the **1a**/O$_2$ reaction were studied by following the disappeareance of **1a** at 630 nm. The absorbance−time profiles were fitted to a single-exponential equation. When [PMe$_2$Ph] and [**1a**] were kept at 6.3 and 0.025 mM, respectively, the observed rate constants were linearly proportional to [O$_2$] in the range 0.31−1.6 mM. The effect of PMe$_2$Ph was studied in the presence of 0.67 mM O$_2$ and 0.048 mM **1a**. As [PMe$_2$Ph] varied from 7.7 to 57 mM, the observed rate constants were inversely proportional to [PMe$_2$Ph], Figure 1. The reactions of **1f** and **1h** with O$_2$ were studied by using a conventional spectrophotometer, whereas the reaction of **1d**/O$_2$ was studied by the use of a stopped-flow spectrophotometer.

Trapping Peroxo Intermediate. A solution of **1d** in C$_6$D$_6$ was prepared from MeRe(NAr)$_2$O and a known amount of P(OMe)$_3$. The ^{31}P NMR spectrum was collected after desired amounts of PAr$_3$ and PAr′$_3$ were added. Molecular oxygen was then introduced, and the reaction was followed using NMR techniques. The amount of each product is limited by the concentration of O$_2$ in solution. Since the equilibration of O$_2$ between the gas and the liquid phases is slow, it is necessary to shake the sample thoroughly a few times before each measurement. The intensities of the ^{31}P resonances were integrated. The plot of ln [PAr$_3$]$_t$ vs ln [PAr′$_3$]$_t$ is linear, Figure 2. The slope of the plot (see the Supporting Information) is $k_{Ar}/k_{Ar'}$ according to Scheme 2.

(8) Fogg, P. G. T.; Gerrard, W. *Solubility of Gases in Liquids*; John Wiley & Sons: Chichester, 1991; pp 292.

Scheme 2

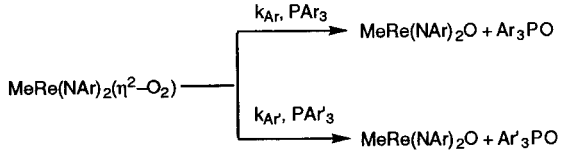

Ligand Exchange. The following general procedure was used to measure the equilibrium constants of the ligand exchange reactions, eqs 1 and 2. A known amount of the incoming ligand PY′$_3$ was added into an NMR tube that contained a toluene-d_8 solution of known amounts of MeRe(NAr)$_2$(PY$_3$)$_2$ and PY$_3$. The ^{31}P{^{1}H} NMR spectrum was then measured at 243 K. These steps were repeated at least three times at different concentrations of PY′$_3$. Intensities of the signals for MeRe(NAr)$_2$(PY$_3$)$_2$, MeRe(NAr)$_2$(PY$_3$)(PY′$_3$), and MeRe(NAr)$_2$(PY′$_3$)$_2$ were used to calculate the equilibrium constants K_1 and K_2. The values of K_1 and K_2 remained the same as the relaxation times used for the collection of the ^{31}P spectra were varied from 1 to 5 s in the case of PY$_3$ = PMe$_3$ and PY′$_3$ = PMe$_2$Ph. Within the experimental error, K_1 and K_2 stayed the same when they were calculated from the intensities of the ^{1}H NMR spectra. For PY$_3$ = P(OMe)$_3$ and PY′$_3$ = P(OEt)$_3$, the ratio of [PY$_3$]$_{tot}$ to [PY′$_3$]$_{tot}$ based on the integration was in agreement with the ratio calculated on the basis of the amounts added, validating the use of calibrated intensities to obtain equilibrium concentrations. Values of K_1 and K_2 for the **1e**/P(OMe)$_3$ reaction were constant as [P(OMe)$_3$] was varied from 0.060 to 0.56 M; see Figure S1 (Supporting Information). The experimental equilibrium constants are summarized in Table 1. The complex MeRe(NAr)$_2${P(OMe)$_3$}{P(OEt)Ph$_2$} was

$$\mathrm{MeRe(NAr)_2(PY_3)_2 + PY'_3 \rightleftarrows MeRe(NAr)_2(PY_3)(PY'_3) + PY_3} \quad (K_1) \quad (1)$$

$$\mathrm{MeRe(NAr)_2(PY_3)(PY'_3) + PY'_3 \rightleftarrows MeRe(NAr)_2(PY'_3)_2 + PY_3} \quad (K_2) \quad (2)$$

detected from the reaction of **1d** with P(OEt)Ph$_2$ at 226 K. Further exchange to yield MeRe(NAr)$_2${P(OEt)Ph$_2$}$_2$ was not observed in the presence of 0.18 M of P(OEt)Ph$_2$ and 0.010 M of P(OMe)$_3$. Similarly, the fully exchanged species for the **1d**/PMePh$_2$ reaction was not observed even with a large excess of PMePh$_2$, 0.35 M. In the case of PPh$_3$, not even the mixed complex MeRe(NAr)$_2${P(OMe)$_3$}(PPh$_3$) was detected, indicating a very small affinity of PPh$_3$ toward Re^V. Assuming the mixed complex is less than 5%, a limit of $K_1 < 0.017$ for the reaction of **1d**/PPh$_3$ can be estimated.

Results

Ligand Exchange. When a different ligand, PY′$_3$, was added to a solution of MeRe(NAr)$_2$(PY$_3$)$_2$ (**1**), the ligand exchange processes, eqs 1 and 2, were observed and conveniently studied by NMR techniques. For example, after 54 mM PMe$_2$Ph was added into a C$_6$D$_6$ solution containing 7.5 mM **1f** and 30 mM PMe$_3$ at 283 K, the ^{1}H NMR spectrum showed a decrease in the intensity of the triplet at 2.75 ppm for C*H*$_3$Re of **1f** and the appearance of a new triplet at 2.57 ppm. The new triplet increased in intensity as more PMe$_2$Ph was added, and another triplet at 2.38 ppm due to C*H*$_3$Re of **1a** appeared at 380 mM PMe$_2$Ph, Figure S2 (Supporting Information). Furthermore, the corresponding ^{13}C resonance for the unidentified triplet is at −29.5 ppm, between −31.8 and −27.5 ppm for *C*H$_3$Re of **1f** and **1a**, respectively. On the basis of the above spectroscopic information and the ^{31}P NMR data, the new species was assigned as the mixed-ligand complex MeRe(NAr)$_2$(PMe$_3$)(PMe$_2$Ph). Figure S3 (Supporting Information) shows the ^{31}P{^{1}H} NMR spectra of the exchange reaction between **1d** and PMe$_2$Ph. It is worth

Table 1. Summary of Equilibrium Constants for the Stepwise and Overall Substitution Reactions of $MeRe(NAr)_2(PY_3)_2$ (**1**) and PY'_3[a]

PY_3	PY'_3	K_1	K_2	β_2
$P(OMe)_3$	PMe_2Ph	98 ± 5	18 ± 2	1800 ± 200
$P(OMe)_3$	$PMePh_2$	0.28 ± 0.02		
$P(OMe)_3$	PPh_3	<0.017		
$P(OMe)_3$	$P(OMe)_2Ph$	15 ± 2	2.5 ± 0.1	38 ± 5
$P(OMe)_3$	$P(OEt)_3$	3.3 ± 0.1	0.72 ± 0.04	2.4 ± 0.2
$P(OMe)_3$	$P(OEt)Ph_2$	0.13 ± 0.01[b]		
$P(OEt)_3$	$P(OMe)_2Ph$	11 ± 1	1.4 ± 0.1	15 ± 2
$P(OEt)_3$	PEt_3	26 ± 2	0.36 ± 0.02	9.4 ± 0.9
PMe_3	$P(OMe)_2Ph$	0.011 ± 0.001	$(5.6 \pm 0.3) \times 10^{-4}$	$(6.1 \pm 0.6) \times 10^{-6}$
PMe_3	PMe_2Ph	0.045 ± 0.002	$(6.9 \pm 0.3) \times 10^{-3}$	$(3.3 \pm 0.2) \times 10^{-4}$
PMe_3	dmpe	0.37 ± 0.02	0.078 ± 0.006	0.029 ± 0.003

[a] In toluene-d_8 at 243 K. [b] In toluene-d_8 at 226 K.

noting that the coupling constant between the two phosphines in $MeRe(NAr)_2\{P(OMe)_3\}(PMe_2Ph)$ is 668 Hz. Very large coupling constants have also been observed in other $MeRe(NAr)_2(PY_3)(PY'_3)$ complexes, Table S1 (Supporting Information). The value of $^2J_{PP}$ varies from 491 Hz for $MeRe(NAr)_2(PMe_3)(PMe_2Ph)$ to 923 Hz for $MeRe(NAr)_2\{P(OMe)_3\}\{P(OEt)_3\}$.

A dynamic process, eq 3, has been established by variable temperature ^1H and $^{31}P\{^1H\}$ NMR studies.[7] The rate of the equilibration depends on the nature of the ligand. For PMe_3 and dmpe, the equilibrating rates were slow on the NMR time scale at 298 K and sharp resonances were observed. However, for PMe_2Ph, $P(OMe)_2Ph$, $P(OMe)_3$, and $P(OEt)Ph_2$ the solution needed to be cooled down to 283, 253, 243, and 223 K, respectively, in order to see a sharp signal for the coordinated phosphines in **1**. On the basis of the coalescence temperature, the binding ability of PY_3 toward Re^V decreases in the following series: $PMe_3 \sim$ dmpe $> PMe_2Ph > P(OMe)_2Ph \sim PEt_3 > P(OEt)_3 \sim P(OMe)_3 > P(OMe)Ph_2$. This order agrees with the results of the quantitative equilibrium studies (see below).

$$MeRe(NAr)_2(PY_3)_2 \rightleftarrows MeRe(NAr)_2(PY_3) + PY_3 \quad (3)$$

Equilibrium Constants. Because of the exchange reaction shown in eq 3, the ^{31}P-signals for some of the Re^V complexes could be observed only at low temperature. For experimental convenience and data comparison, most of the equilibrium constants of eqs 1 and 2 were measured in toluene-d_8 at 243 K except for the reaction of **1d** with $P(OEt)Ph_2$ where K_1 was measured at 226 K. A summary of the experimental values of K_1, K_2, and β_2 (K_1K_2) is given in Table 1. In all of the cases, $K_1 \geq 4K_2$. This is akin to the situation for a dicarboxylic acid: statistical arguments provide the limit $K_1 \geq 4K_2$.[9−11] The equilibrium constant β_2 for reactions that are not listed in Table 1 can be calculated by the use of the data determined experimentally. Since only the K_1 values could be determined for the reactions of **1d** with $PMePh_2$ and $P(OEt)Ph_2$, the corresponding β_2 values are not known. If, however, one assumes $K_2 \leq K_1/4$, as noted above, the following β_2 values for the reactions of **1d** and PY_3 were obtained: $PY_3 = PMe_3$ (6×10^6) > dmpe (1.7×10^6) > PMe_2Ph (1.8×10^3) > $P(OMe)_2Ph$ (38) > PEt_3 (22) > $P(OEt)_3$ (2.4) > $PMePh_2$ ($<2 \times 10^{-2}$, est) > $P(OEt)Ph_2$ ($<4 \times 10^{-3}$, est) > PPh_3 (7×10^{-5}, est).

The self-consistency of the data given in Table 1 can be tested. For example, a β_2 value of 750 ± 99 for the **1e**/PMe_2Ph reaction was calculated from the experimental data for the **1e**/$P(OMe)_3$ and **1d**/PMe_2Ph reactions. Another value, 700 ± 140, was calculated from the data for the **1e**/$P(OMe)_2Ph$ and **1c**/PMe_2Ph reactions. The congruity was also shown for the **1d**/$P(OEt)_3$ reaction. The calculated value is $\beta_2 = 2.5 \pm 0.5$ from the data for the **1c**/$P(OMe)_3$ and **1c**/$P(OEt)_3$ reactions, which agrees with the experimental value, 2.4 ± 0.2.

Table 2. Summary of the Observed Rate Constants for the Reactions of $MeRe(NAr)_2(PY_3)_2$ (**1**) and O_2[a]

PY_3	k_{obs} (K_3k_7)/s^{-1}
$P(OMe)_3$	45 ± 3
PMe_2Ph	0.78 ± 0.02
dmpe	0.044 ± 0.003
PMe_3	0.0078 ± 0.0006

[a] In benzene at 298 K.

The effect of temperature on the equilibrium constants was studied for the **1d**/$PMePh_2$ reaction. From 226 to 253 K, K_1 increases from 0.28 to 0.42, Figure S4 (Supporting Information). The values are $\Delta H° = 7.0 \pm 0.3$ kJ mol^{-1} and $\Delta S° = 21 \pm 1$ J K^{-1} mol^{-1} for the **1d**/$PMePh_2$ reaction. The **1f**/PMe_2Ph reaction showed a similar small temperature effect on K_1; $\Delta H° = 6.7 \pm 0.5$ kJ mol^{-1} and $\Delta S° = -2 \pm 1.7$ J K^{-1} mol^{-1}. Stahl and Ernst have reported a small temperature effect, $\Delta H° = 12$ kJ mol^{-1}, for phosphine exchange with $Ti(2,4\text{-}C_7H_{11})_2(PF_3)$/$PMe_3$.[12]

Reactions of 1 with O_2. ^1H and $^{31}P\{^1H\}$ NMR studies reveal that the reaction between **1a** and O_2 takes place rapidly according to eq 4. The formation of PMe_2Ph in eq 4 is consistent with the fact that reaction 5 is very slow for PMe_2Ph.[7] In the presence of excess O_2 the observed rate constant is first-order with respect to $[O_2]$ and inverse-first-order with respect to $[PMe_2Ph]$. The reactions of O_2 with **1d**, **1f**, and **1h** also occur according to eq 4 and show the same concentration dependences. A summary of the kinetic data is given in Table 2. When the reaction of **1d** and a limiting amount of O_2 was carried out in the presence of an excess of $P(OMe)_3$, the absorbance at 580 nm decreased immediately. After a delay, the absorbance was restored to the original level. When $P(OMe)_3$ was kept constant, the delay lengthened as the $[O_2]$ increased, Figure 3. Kinetic analyses for the rising part of Figure 3 agreed with the data obtained from studies of reaction 5 in the absence of O_2.[7]

$$MeRe(NAr)_2(PY_3)_2 + O_2 \rightarrow MeRe(NAr)_2O + Y_3PO + PY_3 \quad (4)$$

$$MeRe(NAr)_2O + 3PY_3 \rightarrow MeRe(NAr)_2(PY_3)_2 + Y_3PO \quad (5)$$

(9) March, J. *Advanced Organic Chemistry*, 4th ed.; Wiley: New York, 1992; pp 266−267.
(10) Eberson, L. Acidity and hydrogen bonding of carboxyl groups. In *The Chemistry of Carboxylic Acids and Esters*; Patai, S., Ed.; Interscience: New York, 1969; pp 211−293.
(11) Adamov, A. A.; Nesterova, R. G.; Freidlin, G. N.; Shirobokova, O. I. *Zh. Obshch. Khim.* **1977**, *47*, 1900−1904.
(12) Stahl, L.; Ernst, R. D. *J. Am. Chem. Soc.* **1987**, *109*, 5673.

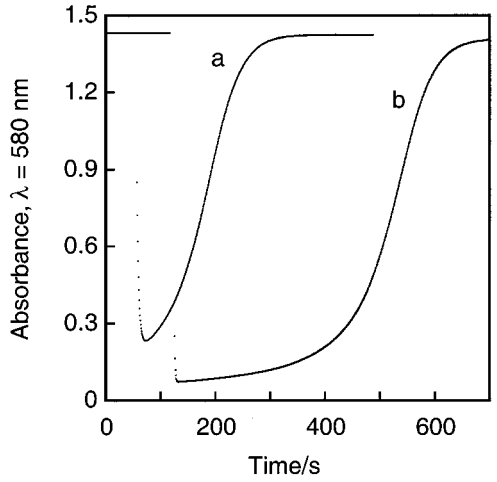

Figure 3. Absorbance−time profiles for the reaction of $MeRe(NAr)_2\{P(OMe)_3\}_2$ and O_2. $[O_2] = 0.4$ mM (a) and 1.4 mM (b).

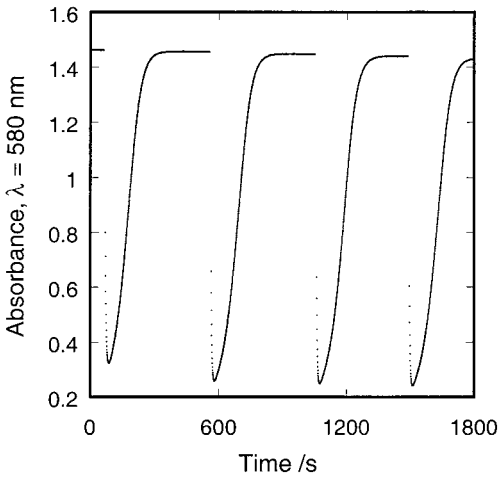

Figure 4. Large absorbance−time excursions during the catalytic oxidation of $P(OMe)_3$ (52 mM) by O_2 in the presence of 0.11 mM $MeRe(NAr)_2O$. The absorbance of the catalyst falls quickly when O_2 is added and then recovers when the oxygen supply is exhausted. The experiment can be repeated indefinitely by addition of further oxygen as long as the phosphite remains.

Catalytic Oxidation with O_2. Upon addition of 0.4 mM O_2 to a 0.11 mM **1d** in benzene solution containing 52 mM $P(OMe)_3$, the color quickly faded and then regenerated. As shown in Figure 4, this process could be repeated many times by the intermittent replenishment of the O_2 until $P(OMe)_3$ had been entirely consumed. NMR spectroscopy showed that $(MeO)_3PO$ is the only product after the reaction. It has been observed that the rate of eq 5 increases significantly when alkoxy groups are bound to phosphorus. From eqs 4 and 5 one can predict that $MeRe(NAr)_2O$ will be an efficient catalyst for the oxidations of $P(OR)_nPh_{3-n}$ with molecular oxygen. Indeed, a graph similar to that shown in Figure 4 was obtained when a limiting amount of O_2 was added to a solution of $MeRe(NAr)_2O$ and excess $P(OR)_nPh_{3-n}$ (R = Me. Et; $n = 1-3$). Noticeable decomposition of catalyst was observed for the reactions with $P(OR)_nPh_{3-n}$ (R = Me, Et; $n = 1, 2$). In the case of triaryl phosphines, the catalytic activity of $MeRe(NAr)_2O$ is insignificant. However, $MeRe(NAr)_2O$ does catalyze the oxidation of PPh_3 with O_2 when $P(OMe)_3$ is present. The amount of oxidized product $(MeO)_3PO$ was slightly higher than Ph_3PO when the reaction was carried out initially with similar amounts of $P(OMe)_3$ and PPh_3.

Table 3. Relative Reactivity of PAr_3 toward the Proposed Intermediate $MeRe(NAr)_2(\eta^2\text{-}O_2)$ and the Known Compound $MeReO_2(\eta^2\text{-}O_2)$

		rel reactivity	
PAr_3	σ	$MeRe(NAr)_2(\eta^2\text{-}O_2)$	$MeReO_2(\eta^2\text{-}O_2)^a$
$P(4\text{-}MeOC_6H_4)_3$	−0.27	1.65	
$P(4\text{-}MeC_6H_4)_3$	−0.17	1.12	1.29
PPh_3	0	1	1b
$P(4\text{-}FC_6H_4)_3$	0.06	0.899	
$P(4\text{-}ClC_6H_4)_3$	0.23	0.823	0.658
$P(4\text{-}CF_3C_6H_4)_3$	0.54	0.590	0.466

[a] Reference 13. [b] The second-order rate constant is 7.3×10^5 L mol^{-1} s^{-1}.[13]

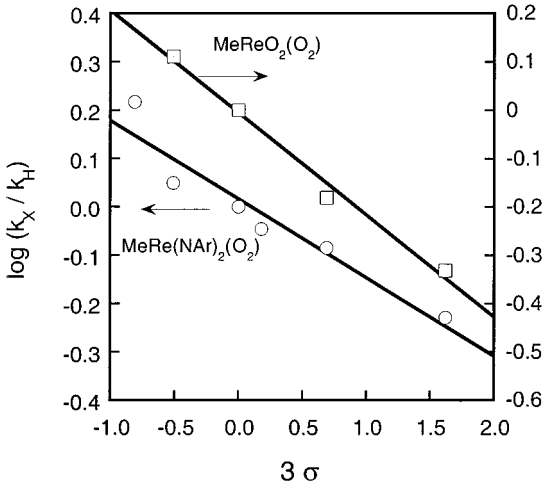

Figure 5. Hammett plot for the reaction of PAr_3 with $MeRe(NAr)_2(\eta^2\text{-}O_2)$ (open circles) and $MeReO_2(\eta^2\text{-}O_2)$ (open squares).

A Peroxo Intermediate. The preceding results suggest that an intermediate is formed in the $MeRe(NAr)_2O$-catalyzed oxidation of phosphines with molecular oxygen that can effectively transfer an oxygen atom to PPh_3. It is conceivably a peroxo intermediate because related complexes are known to react with PAr_3.[13] The active intermediate in the current system was investigated by trapping it with a pair of triaryl phopsphines. The relative reactivities of phosphines toward the proposed intermediate $MeRe(NAr)_2(\eta^2\text{-}O_2)$ and the known compound $MeReO_2(\eta^2\text{-}O_2)$ are given in Table 3. The reaction constants derived from Hammett plots are −0.16 and −0.22 for $MeRe(NAr)_2(\eta^2\text{-}O_2)$ and $MeReO_2(\eta^2\text{-}O_2)$, respectively, Figure 5.

A variety of phosphines, $P(OR)_nPh_{3-n}$ and PR_nPh_{3-n}, have been studied with $MeRe(NAr)_2O$.[7] The reactivity of a number of PAr_3 toward $MeReO_2(\eta^2\text{-}O_2)$ has also been reported.[13] To understand better the oxo-transfer reactions involving metal−oxo and metal−peroxo complexes, the reactions of $P(OMe)_3$, $P(OMe)_2Ph$, $P(OMe)Ph_2$, and PPh_3 with $MeReO(\eta^2\text{-}O_2)_2$ in CH_3CN ($[H_2O] = 0.2$ M) were studied by monitoring the disappearance of $MeReO(\eta^2\text{-}O_2)_2$ at 360 nm by the use of a stopped-flow spectrophotometer. The second-order rate constant for the reaction with $P(OMe)_3$, from Figure S5 (Supporting Information), is $(3.1 \pm 0.1) \times 10^4$ L mol^{-1} s^{-1} at 25 °C. As shown in Table 4, the rate constant increases in the order $P(OMe)_3 < P(OMe)_2Ph < P(OMe)Ph_2 < PPh_3$.

Discussion

***trans*-$MeRe(NAr)_2(PY_3)(PY'_3)$.** The crystal structures of **1a** and **1h** reveal that the two phosphines are trans to each other

(13) Abu-Omar, M. M.; Espenson, J. H. *J. Am. Chem. Soc.* **1995**, *117*, 272.

Table 4. Second-Order Rate Constants ($/10^5$ L mol^{-1} s^{-1}) for the Oxo-Transfer Reactions between PY_3 and $MeReO(\eta^2\text{-}O_2)_2$

PY_3	PPh_3	$P(OMe)Ph_2$	$P(OMe)_2Ph$	$P(OMe)_3$	
$MeReO(\eta^2\text{-}O_2)_2$[a]	10 ± 1	4.2 ± 0.3	2.5 ± 0.2	0.31 ± 0.01	this work
$MeReO(\eta^2\text{-}O_2)_2$[b]	21.6 ± 0.5				*c*

[a] In CH_3CN. [b] In 0.10 M $HClO_4$ solution of H_2O/CH_3CN (v:v = 50:50). [c] Reference 13.

($\angle$(P−Re−P) = 176°).[7] The trans configuration of phosphines likely persists in the mixed complexes as supported by the large coupling constant, $^2J_{PP} > 491$ Hz, Table S1. Large P−P coupling constants have been observed for *trans*-$Mo_2Cl_2(NH_2R)(PY_3)(PY'_3)$, where $\angle$(P−Mo−P) = 155°.[14] A $^2J_{PP}$ coupling constant >500 Hz has been reported in the systems of *trans*-$MX_2(PY_3)(PY'_3)$ (M = Pd, Pt; X = Cl, I).[15,16] The P−M−P angles here are likely greater than 170° as crystallographically found in the analogous compounds like *trans*-$MLL'(PY_3)_2$.[17−20] Many examples have been reported to show that P−P coupling is larger for trans groups than for cis.[21−23]

Binding to Re^V. Phosphines display a wide range of steric and electronic effects on coordination to transition metals.[24] The data in Table 1 clearly demonstrate that both factors govern the binding ability of PY_3 toward Re^V. Phosphines with large cone angles and weak basicities, such as $P(OEt)Ph_2$ and PPh_3, show little affinity for Re^V. On the other hand, phosphines with small cone angles and strong basicities, such as PMe_3 and dmpe, form strong bonds to Re^V. Since the steric demands measured by Tolman's cone angle for PMe_3 and $P(OMe)_2Ph$ are similar, θ = 118° and 120°, respectively,[25] the electronic effect can be examined by comparing their binding ability toward Re^V. Five orders of mangitude separate the equilibrium constants for the reactions of **1d** with PMe_3 ($\beta_{2d} = 6 \times 10^6$) and with $P(OMe)_2Ph$ ($\beta_{2d} = 38$). This is in line with the great differences in their basicities, pK_a = 8.65 and 2.64, respectively. Evidently the electronic effect is not the dominant factor in this sterically crowded system. For example, even though PEt_3 (pK_a = 8.69) is much more basic than $P(OMe)_2Ph$ (pK_a = 2.64), the equilibrium constant, β_2, between **1g** and PEt_3 is only 6. The very small difference in preference between PEt_3 and $P(OMe)_2Ph$ by Re^V is attributed to the larger steric demand by PEt_3 (θ = 132°) than that of $P(OMe)_2Ph$ (θ = 120°). Also, the value of 0.36 for K_{1d} of the **1d**/$PMePh_2$ reaction is due to the steric (θ = 108° and 136° for $P(OMe)_3$ and $PMePh_2$, respectively) rather than the electronic effect (pK_a = 2.60 and 4.57 for $P(OMe)_3$ and $PMePh_2$, respectively). Andersen and co-workers have used the steric effect to explain the trend of $PMe_3 < PMe_2Ph \ll PEt_3$ for the dissociation equilibrium constant of $Mo_2Me_4(PY_3)_4$.[26] The same trend was also observed by Stahl and Ernst in the $Ti(2,4\text{-}C_7H_{11})_2(PY_3)$ system, and rationalized by steric effects.[12] Because of the roles played by both steric and electronic factors in the current system, the correlation between the equilibrium constants (β_{2d} for the **1d**/PY_3 reaction) and Tolman's electronic (χ)[27] or steric (θ)[25,28] parameters is poor for the entire series of compounds investigated. A better correlation was observed when both factors were considered. Plots of log β_{2d} and pK_a of PY_3 against the calculated values according to eq 6 are given in Figure S6 (Supporting Information). The fitting parameters are $a = -0.47 \pm 0.10$, $b = -0.29 \pm 0.05$, and $c = 43 \pm 6.7$ for log β_{2d}; and $a = -0.53 \pm 0.03$, $b = -0.13 \pm 0.015$, and $c = 28 \pm 2$ for pK_a. Extensive studies on correlations involving both χ and θ have been carried out by Giering et al.[27]

$$\log\beta_{2d} \quad \text{or} \quad pK_a = a\chi + b\theta + c \tag{6}$$

The kinetic reactivity of PY_3 toward $MeRe(NAr)_2O$, the formation of **1**, follows the order $P(OR)_nPh_{3-n} \gg PR_nPh_{3-n}$. However, the thermodynamic stability of **1** follows the opposite order: $PR_nPh_{3-n} > P(OR)_nPh_{3-n}$.

Mechanism for the Exchange Reactions. The fast ligand exchange processes, eqs 1 and 2, and the instability of **1** in solution, eq 3, preclude an easy measurement of the exchange rates as a function of the incoming ligands and activation entropies for the exchange reactions. Nevertheless, a dissociative mechanism involving a transient 4-coordinated species $MeRe(NAr)_2(PY_3)$, eq 3, likely operates in this sterically crowded system. The coordinatively unsaturated compound $MeRe(NAr)_2(PY_3)$ reacts with the incoming ligand PY'_3 to give a mixed product or is trapped by molecular oxygen to give a peroxo complex (see below). Mechanistic studies have shown that the ligand exchange reactions for the 16e systems, $Mo_2Me_4(PY_3)_4$[26] and $Ti(2,4\text{-}C_7H_{11})_2(PY_3)$,[12] occur via a dissociative mechanism. An interchange dissociative mechanism has been demonstrated in the case of $Mo_2Cl_4(PY_3)_4$.[29]

Catalytic Oxidation with O_2. Oxidations of tertiary phosphines with molecular oxygen catalyzed by transition metal complexes are known.[30−33] However, the mechanistic details, such as the roles of peroxo− and oxo−metal complexes, are still lacking. Dinuclear metal peroxides have been proposed in the catalytic cycles;[32,34] however, the oxo-transfer step is believed to occur between a high-valent metal−oxo complex

(14) Cotton, F. A.; Dikarev, E. V.; Herrero, S. *Inorg. Chem.* **2000**, *39*, 609.
(15) Goodfellow, R. G. *Chem. Commun.* **1968**, 114.
(16) Hitchcock, P. B.; Jacobson, B.; Pidcock, A. *J. Chem. Soc., Dalton Trans.* **1977**, 2038.
(17) Schneider, M. L.; Shearer, H. M. M. *J. Chem. Soc., Dalton Trans.* **1973**, 354.
(18) Huffman, J. C.; Laurent, M. P.; Kochi, J. K. *Inorg. Chem.* **1977**, *16*, 2369.
(19) Bennett, M. A.; Robertson, G. B.; Rokicki, A.; Wickramasinghe, W. A. *J. Am. Chem. Soc.* **1988**, *110*, 7098.
(20) Cowan, R. L.; Trogler, W. C. *J. Am. Chem. Soc.* **1989**, *111*, 4750.
(21) Pregosin, P. S.; Kunz, R. W. In *NMR Basic Principles and Progress*; Diehl, P., Fluck, E., Kosfeld, R., Eds.; Springer-Verlag: Berlin, 1979; Vol. 16, pp 1−156.
(22) *Phosphorus-31 NMR Spectroscopy in Stereochemical Analysis*; Verkade, J. G., Quin, L. D., Eds.; VCH: Deerfield Beach, 1987.
(23) Lindner, E.; Mayer, H. A.; Mockel, A. Applications of ^{31}P NMR Spectroscopy in the Investigation of the Dynamic Behavior of Five-Membered Ether-Phosphine Metal Complexes. In *Phosphorus-31 NMR Spectral Properties in Compound Characterization and Structural Analysis*; Quin, L. D., Verkade, J. G., Eds.; VCH: New York, 1994; p 215.
(24) Dias, P. B.; Minas de Piedade, M. E.; Martinho Simoes, J. A. *Coord. Chem. Rev.* **1994**, *135/136*, 737.
(25) Tolman, C. A. *Chem. Rev.* **1977**, *77*, 313.
(26) Girolami, G. S.; Mainz, V. V.; Andersen, R. A. *J. Am. Chem. Soc.* **1981**, *103*, 3953.
(27) Liu, H.-Y.; Eriks, K.; Prock, A.; Giering, W. P. *Organometallics* **1990**, *9*, 1758.
(28) Bartik, T.; Himmler, T.; Schulte, H.-G.; Seevogel, K. *J. Organomet. Chem.* **1984**, *272*, 29.
(29) Chrisholm, M. H.; McInnes, J. M. *J. Chem. Soc., Dalton Trans.* **1997**, 2735.
(30) Schmidt, D. D.; Yoke, J. T. *J. Am. Chem. Soc.* **1971**, *93*, 637.
(31) Monica, G. L.; Cenini, S. *J. Chem Soc., Dalton Trans.* **1980**, 1145.
(32) Khan, M. M. T.; Chatterjee, D.; Siddiqui, M. R. H.; Bhatt, S. D.; Bajaj, H. C.; Venkatasubramanian, K.; Moiz, M. A. *Polyhedron* **1993**, *12*, 1443.
(33) Heinze, K.; Huttner, G.; Zsolnai, L. *Chem. Ber.* **1997**, *130*, 1393.
(34) Cheng, S. Y. S.; James, B. R. *J. Mol. Catal.* **1997**, *117*, 91.

Scheme 3

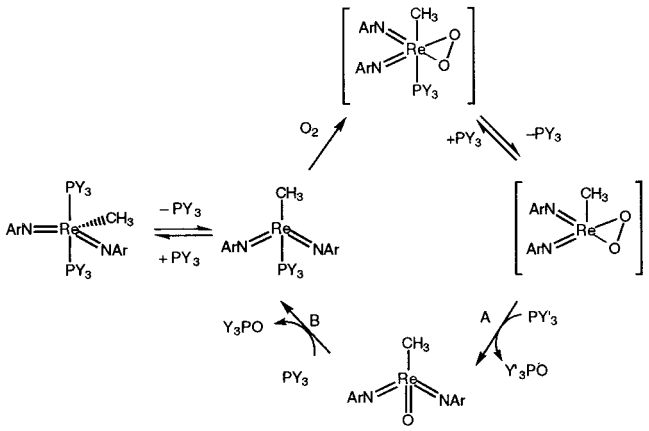

and phosphines. The most convincing evidence is the isotope distribution in the phosphine product of the $[Os(N)R_2(\mu\text{-}O)_2\text{-}Cr^{16}O_2]^{+}/^{18}O_2$/dppe reaction.[35] The possibilities that the O_2 adducts of monomeric and dimeric cobalt phosphine complexes undergo the oxo-transfer reaction have been briefly discussed by Huttner and co-workers.[33] Halpern and co-workers have domonstrated that a peroxo intermediate, $Pt(PPh_3)_2(O_2)$, is involved in the catalysis of the autoxidation of PPh_3 by $Pt(PPh_3)_3$.[36] The catalytic cycle proposed for the current system, Scheme 3, can be divided into two parts. First, a Re^{V} species is generated and $(MeO)_3PO$ formed, step B. This step has been studied independently.[7] The reaction of $MeRe(NAr)_2O$ with PAr_3 is very sluggish, regardless of the presence or absence of O_2; thus the formation of Ar_3PO from the first stage is negligible. The second part contains the production of the peroxo−Re^{VII} complex and the formation of Ar_3PO. The data for the oxo-transfer reaction between $MeReO(\eta^2\text{-}O_2)_2$ and $P(OMe)_nPh_{3-n}$ in Table 4 suggest that the formation of $(MeO)_3PO$ is insignificant during the second stage when the amounts of $P(OMe)_3$ and PAr_3 are comparable. As predicted by this model, $^{31}P\{^1H\}$ NMR studies have shown that the amount of $(MeO)_3PO$ is nearly the same as the amount of $OPAr_3$. The similarity in relative reactivity between $MeRe(NAr)_2(\eta^2\text{-}O_2)$ and the known compound $MeReO_2(\eta^2\text{-}O_2)$, Figure 5, supports the postulated peroxo intermediate. Under the experimental conditions neither PAr_3 nor PAr'_3 will replace $P(OMe)_3$ in **1d** (see above).

Kinetic studies for the reactions of $MeRe(NAr)_2(PY_3)_2$ and O_2 also support the proposed mechanism. Following a fast equilibrium, eq 3, the step of the O_2 reaction is likely the rate-controlling step; the subsequent reactions will not provide any kinetic contribution. Combining eqs 3 and 7, and assuming eq 3 is a fast equilibrium, the corresponding rate law, eq 8, is obtained when large excesses of O_2 and PY_3 are used. With $[PY_3] \gg K_3$, the rate law can be simplified to the form observed experimentally, such that $k_\psi = K_3k_7$. A reaction of O_2 with **1d** that is much faster than the one with **1f** may result from the difference of K_3. This is consistent with the results of the equilibrium studies, given that PMe_3 is a much better ligand than $P(OMe)_3$ toward Re^{V}.

$$CH_3Re(NAr)_2(PY_3) + O_2 \rightarrow CH_3Re(NAr)_2O + Y_3PO \quad (7)$$

$$k_\psi = \frac{K_3k_7[O_2]}{K_3 + [PY_3]} \quad (8)$$

Conclusion

The current system affords an interesting comparison of the reactivities between oxo− and peroxo−rhenium complexes toward phosphines. The reactivities of phosphines follow the order $P(OR)_nPh_{3-n} > PR_nPh_{3-n}$ in the oxo-transfer reactions with $L_nRe^{VII}{=}O$, whereas the opposite order is observed with $L_nRe^{VII}(\eta^2\text{-}O_2)$. Apparently, π-acidity plays a dominant role in the oxo-transfer reactions with Re═O whereas σ-basicity dominates with $Re(\eta^2\text{-}O_2)$. The influence of the basicity of phosphine is also shown in its coordination in $MeRe^{V}(NAr)_2(PY_3)_2$. The more basic PY_3 is, the more strongly it binds to Re^{V}. However, the steric effect is the dominant factor governing the coordination ability of PY_3.

Acknowledgment. This research was supported by the U.S. Department of Energy, Office of Basic Energy Sciences, Division of Chemical Sciences under Contract W-7405-Eng-82.

Supporting Information Available: Table of the $^{31}P\{^1H\}$ NMR data for $MeRe(NAr)_2(PY_3)(PY'_3)$. Figures for the ^1H and ^{31}P NMR spectra of selected $MeRe(NAr)_2(PY_3)(PY'_3)$ complexes. Kinetic analyses for the trapping experiments and table for the relative reactivity of PY_3 toward $MeRe(NAr)_2(\eta^2\text{-}O_2)$ and $MeReO_2(\eta^2\text{-}O_2)$. This material is available free of charge via the Internet at http://pubs.acs.org.

IC000940K

(35) Shapley, P. A.; Zhang, N.; Allen, J. L.; Pool, D. H.; Liang, H.-C. *J. Am. Chem. Soc.* **2000**, *122*, 1079.
(36) Sen, A.; Halpern, J. *J. Am. Chem. Soc.* **1977**, *99*, 8337.